



Aphotic N₂ fixation along an oligotrophic to ultraoligotrophic transect in the Western Tropical South Pacific Ocean

Mar Benavides^{1,2}, Katyanne M. Shoemaker³, Pia H. Moisander³, Jutta Niggemann⁴, Thorsten Dittmar⁴,
5 Solange Duhamel⁵, Olivier Grosso⁶, Mireille Pujo-Pay⁷, Sandra Hélias-Nunige⁶, Sophie Bonnet¹

¹Aix Marseille Université, CNRS/INSU, Université de Toulon, IRD, Mediterranean Institute of Oceanography (MIO) UM 110, 98848 Nouméa, New Caledonia

²Marine Biology Section, Department of Biology, University of Copenhagen, 3000 Helsingør, Denmark

10 ³Department of Biology, University of Massachusetts Dartmouth, 285 Old Westport Road, North Dartmouth, MA 02747, USA

⁴Research Group for Marine Geochemistry (MPI-ICBM Bridging Group), Institute for Chemistry and Biology of the Marine Environment University of Oldenburg, Carl-von-Ossietzky-Strasse 9-11, D-26129 Oldenburg, Germany

15 ⁵Lamont-Doherty Earth Observatory, Division of Biology and Paleo Environment, Columbia University, PO Box 1000, 61 Route 9W, Palisades, NJ 10964, USA

⁶Aix Marseille Université, CNRS/INSU, Université de Toulon, IRD, Mediterranean Institute of Oceanography (MIO) UM 110, 13288 Marseille, France

20 ⁷Laboratoire d'Océanographie Microbienne – UMR 7321, CNRS - Sorbonne Universités, UPMC Univ Paris 06, Observatoire Océanologique, 66650 Banyuls-sur-mer, France

Correspondence to: Mar Benavides (mar.benavides@bio.ku.dk)

Abstract.

25 The western tropical South Pacific (WTSP) Ocean has been recognized as a global hotspot of dinitrogen (N₂) fixation. Here, as in other marine environments across the oceans, N₂ fixation studies have focused in the sunlit layer. However, studies have confirmed the importance of aphotic N₂ fixation activity, although until now only one had been performed in the WTSP. In order to increase our knowledge of aphotic N₂ fixation in the WTSP, here we measure N₂ fixation rates and identify diazotrophic
30 phylotypes in the mesopelagic layer along a transect spanning from New Caledonia to French Polynesia. Because non-cyanobacterial diazotrophs presumably need external dissolved organic matter (DOM) sources for their nutrition, we also identified DOM compounds using Fourier Transform Ion Cyclotron Mass Spectrometry (FTICRMS). N₂ fixation rates were low (average 0.63 ± 0.07 nmol N L⁻¹ d⁻¹), but consistently detected across all depths and stations, representing ~6-88% of photic N₂ fixation.
35 N₂ fixation rates were not significantly correlated to DOM compounds. The analysis of *nifH* gene



amplicons revealed a wide diversity of non-cyanobacterial diazotrophs, majorly matching clusters 1 and 3. Interestingly, a distinct phylotype from the major *nifH* subcluster 1G dominated at 650 dbar, coinciding with the oxygenated Sub-Antarctic Mode Water (SAMW). This consistent pattern suggests that the distribution of aphotic diazotroph communities is to some extent controlled by water mass structure. While the data available is still too scarce to elucidate the distribution and controls of mesopelagic non-cyanobacterial diazotrophs in the WTSP, their prevalence in the mesopelagic layer and the consistent detection of active N₂ fixation activity at all depths sampled during our study suggest that aphotic N₂ fixation may contribute significantly to fixed nitrogen inputs in this area.

10 **1 Introduction**

Pelagic N₂ fixation is considered the greatest input of fixed nitrogen to the oceans, adding up to ~100-107 Tg N per year (Codispoti, 2007; Galloway et al., 2004; Gruber and Galloway, 2008; Jickells et al., 2017). In the sunlit layer of the warm oligotrophic tropical and subtropical oceans, cyanobacterial diazotrophs such as *Trichodesmium*, UCYN-B and diatom-diazotroph associations (DDAs) dominate fixed nitrogen inputs via N₂ fixation (Capone et al., 1997; Montoya et al., 2004). In colder and less oligotrophic waters at higher latitudes, other diazotrophs including UCYN-A and non-cyanobacterial groups such as Gamma A may be more competitive (Bonnet et al., 2015; Langlois et al., 2015; Moisander et al., 2010; 2014), expanding considerably the latitudinal range where N₂ fixation is considered significant in predictive biogeochemical models. In the past decade, several studies have retrieved *nifH* sequences from the dark ocean, some also accompanied by low N₂ fixation rates (Bonnet et al., 2013; Hamersley et al., 2011; Rahav et al., 2013). Due to the immense volume of the dark ocean, aphotic N₂ fixation could influence the global nitrogen budget substantially. However, the number of published aphotic N₂ fixation rates is scant and our understanding of aphotic diazotrophs' metabolism and ecology of aphotic diazotrophs is still limited, hindering our ability to evaluate their impact on global fixed nitrogen inputs (Moisander et al., 2017).

Non-cyanobacterial diazotrophs span the four established *nifH* gene clusters (Chien and Zinder, 1996), are the most numerous in *nifH* gene databases (Farnelid and Riemann, 2008), and are spread throughout the global ocean (Bonnet et al., 2015; Farnelid et al., 2011; Langlois et al., 2015; Messer et al., 2015). As discussed in Bombar et al. (2016), the growth and activity of non-cyanobacterial diazotrophs may be controlled by (i) the presence of oxygen -because oxygen destroys the nitrogenase enzyme, (ii) the availability of fixed nitrogen because N₂ fixation becomes too energetically expensive when reduced nitrogen forms are readily available in the environment, and (iii) the availability of energy because non-cyanobacterial diazotrophs may not be able to photosynthesize and thus rely on external fixed carbon sources. However, aphotic diazotrophic activity has been found both in oxygen deficient regions such as the oxygen minimum zone of the Eastern Tropical South Pacific (Bonnet et al., 2013; Loescher et al., 2014), and fully oxygenated mesopelagic waters in the Mediterranean Sea



(Benavides et al., 2016; Rahav et al., 2013). Moreover, while fixed nitrogen availability should theoretically shut down N_2 fixation, significant N_2 fixation rates have been measured in nitrate rich mesopelagic waters of the Western Tropical South Pacific (WTSP) (Benavides et al., 2015). Finally, energy is likely made available to heterotrophic non-cyanobacterial diazotrophs through labile dissolved organic matter (DOM). Aphotic N_2 fixation rates have been related to the presence of relatively labile DOM compounds such as transparent exopolymeric particles (TEP) in the WTSP (Benavides et al., 2015), or peptides and unsaturated aliphatics in the Mediterranean Sea (Benavides et al., 2016). The addition of small labile DOM molecules such as carbohydrates or amino acids has been shown to enhance aphotic N_2 fixation in various environments (Benavides et al., 2015; Bonnet et al., 2013; Loescher et al., 2014; Rahav et al., 2013). However, some photic non-cyanobacterial diazotrophs also bear genes for the degradation of refractory DOM compounds (e.g. aromatic hydrocarbons; Bentzon-Tilia et al., 2015). It is thus reasonable to expect that aphotic non-cyanobacterial diazotrophs may be able to exploit diverse DOM sources. Unfortunately, the current lack of genome information from non-cyanobacterial aphotic diazotrophs does not allow us to assess how they are affected by DOM composition and lability.

The WTSP has been recently recognized as a global hotspot of photic N_2 fixation, harboring among the highest N_2 fixation rates ever recorded ($\sim 600 \mu\text{mol N m}^{-2} \text{d}^{-1}$; Bonnet et al., 2017), mostly attributed to *Trichodesmium* and UCYN-B (Berthelot et al., 2017; Bonnet et al., 2015; 2009; Stenegren et al., 2017). To the eastern border of this region, the ultraoligotrophic South Pacific Gyre (GY) has low photic N_2 fixation rates (Raimbault and Garcia, 2008), which have been mainly attributed to small unicellular diazotrophs such as UCYN-A and Gammaproteobacteria (Bonnet et al., 2008; Halm et al., 2012; Stenegren et al., 2017). Despite its potentially immense implications in global fixed nitrogen inputs, the aphotic N_2 fixation potential of the WTSP remains mostly unexplored (Benavides et al., 2015). Here we quantify N_2 fixation in the mesopelagic layer along a ~ 5000 km transect in the WTSP, spanning from oligotrophic to ultraoligotrophic conditions (Moutin et al., 2017).

2 Materials and methods

2.1 Hydrography, nutrients, chlorophyll *a* and dissolved organic carbon

The OUTPACE cruise (Oligotrophy to Ultraoligotrophy South Pacific Experiment; <http://dx.doi.org/10.17600/15000900>) took place onboard the R/V *L'Atalante* from 20 February to 2 April 2015 (i.e. during austral summer), sailing westwards from New Caledonia to French Polynesia (see Figure 2 in Moutin et al., 2017). Temperature, salinity, chlorophyll fluorescence and oxygen data were obtained using a SBE 9plus CTD mounted on a General Oceanics rosette frame fitted with 24 - 12 L Niskin bottles.

Seawater samples were collected with Niskin bottles mounted on a rosette frame at 15 short duration (SD, 8 h) and 3 long duration (LD, 7 days) stations (Moutin et al., 2017). Samples for the



determination of inorganic nutrients nitrate (NO_3^-), nitrite (NO_2^-) and phosphate (PO_4^{3-}) were collected in 20 mL acid-washed polyethylene flasks, poisoned with 1% mercury chloride, and analyzed onshore using a AA3 Bran+Luebbe autoanalyzer. The detection limit for both NO_3^- and PO_4^{3-} was $0.05 \mu\text{M}$. Samples for the determination of dissolved organic carbon (DOC) were collected in combusted glass bottles and immediately filtered through two mounted precombusted (4 h, 450°C) 25 mm GF/F filters (0.7 μm , Whatman) using a custom-made all-glass/teflon filtration syringe system. Filtered seawater was directly collected in precombusted glass ampoules and acidified to pH 2 with orthophosphoric acid. Ampoules were immediately sealed and stored cold (4°C) and in the dark until analyses by high temperature catalytic oxidation on a Shimadzu TOC-L analyzer according to Sohrin et al. (2005). Typical analytical precision is $\pm 0.1 - 0.5$ (SD) or $0.2 - 0.5\%$ (CV). Consensus reference materials (<http://www.rsmas.miami.edu/groups/biogeochem/CRM.html>) were injected every 12 to 17 samples to control for stable operating conditions. Chlorophyll *a* (Chl *a*) concentrations were determined from 500 mL samples filtered through GF/F filters. Chl *a* was extracted in methanol and measured by fluorometry (Herbland et al., 1985).

15

2.2 DOM analysis

Samples for ultra-high resolution mass spectrometry analyses were collected in acid-cleaned 2 L transparent polycarbonate bottles and extracted (solid-phase) via Agilent PPL cartridges as described in Dittmar et al. (2008). After extraction, the cartridges were rinsed with acidified ultrapure water and frozen at -20°C . Subsequently, the samples were dried by flushing with high-purity N_2 and eluted with 6 mL of methanol. The efficiency of the extraction was $47.3 \pm 3.9\%$ on a carbon basis. Methanol extracts were molecularly characterized on a 15 Tesla Fourier-transform ion cyclotron resonance mass spectrometer (Solarix FTICRMS) using an electrospray ionization source in negative mode (Bruker Apollo II). Molecular formulae were ascribed to the detected masses as outlined in Seidel et al. (2014). The aromaticity and unsaturation degree of each compound were evaluated according to its molecular formula and were presented as the modified aromaticity index (AI-mod) and double bond equivalents (DBE), respectively (Koch and Dittmar, 2006). In addition, we ascribed the identified molecular formulae identified to compound groups according to established molar ratios, AI-mod, DBE and heteroatom contents (Seidel et al., 2014). To reveal compositional differences among samples, we performed a principal coordinate analysis (PCoA) on Bray-Curtis distance matrices, including all detected molecular formulae and their respective relative FTICRMS signal intensities. The PCoA scores were correlated against all hydrographic and biological variables measured in our study.

2.3 N_2 fixation rates

Seawater was sampled at each SD station from 200, 500, 650 and 800 dbar in quadruplicate 4.3 L transparent polycarbonate bottles covered with black cloth. Each bottle was spiked with 6 mL of $^{15}\text{N}_2$



gas (98.9% Euriso-top), inverted 20-30 times, and incubated in the dark at 8°C in temperature-regulated incubators onboard. After 24 h of incubation, each pair of bottles were filtered onto separate pre-combusted GF/F filters (treated as duplicates), and stored at -20°C until analyzed with an Integra2 Analyzer, calibrated every ten samples using reference material (IAEA-N1). To obtain accurate N₂ fixation rates we (1) measured the initial $\delta^{15}\text{N}$ of N₂ in the incubation on each incubation bottle by membrane inlet mass spectrometry analyses (MIMS; Kana et al., 1994), (2) collected time zero samples in duplicate at each depth and station to determine the natural $\delta^{15}\text{N}$ of ambient particulate nitrogen (PN), and (3) subtracted blank GF/F PN values from our results. N₂ fixation rates were calculated with the equations of Montoya et al. (1996). Considering the PN linearity limit of the mass spectrometer (2.32 $\mu\text{g N}$), three times the standard deviation of time zero values (natural $\delta^{15}\text{N}$ of PN), our usual filtration volume (8.6 L) and incubation time (24 h), our volumetric N₂ fixation rate detection limit was 0.027 nmol N L⁻¹ d⁻¹. The minimum quantifiable rate calculated using standard propagation of errors via the observed variability between replicate samples was 0.006 nmol N L⁻¹ d⁻¹.

2.4 Flow cytometry

Samples for cell enumeration were collected at the same stations and depths as samples for the quantification of N₂ fixation rates. Samples of 1.8 mL were fixed (0.25% electron microscopy grade paraformaldehyde, w/v) for 10-15 min at room temperature in the dark, flash-frozen in liquid nitrogen and stored at -80°C for later analysis using a BD Influx flow cytometer (BD Biosciences, San Jose, CA, USA). Samples were thawed at room temperature, in the dark, and reference beads (Fluoresbrite, YG, 1 μm) were added to each sample. The non-pigmented bacterioplankton (hereafter bacteria) were discriminated in a sample aliquot stained with SYBR Green I DNA dye (1:10,000 final). Because the *Prochlorococcus* population cannot be uniquely distinguished in the SYBR stained samples in the upper water column, bacteria were determined as the difference between the total cell numbers of the SYBR stained sample and *Prochlorococcus* enumerated in unstained samples. Particles were excited at 488 nm (plus 457 nm for unstained samples) and forward (<15°) scatter (FSC), green fluorescence (530/40 nm), orange fluorescence (580/30 nm) and red fluorescence (>650 nm) emissions were measured. Bacteria were discriminated based on their green fluorescence and FSC characteristics. Cytograms were analyzed using FCS Express 6 Flow Cytometry Software (De Novo Software, CA, US).

2.5 DNA extraction, sequencing, and sequence analysis

Samples for DNA extraction were collected in duplicate in 4.3 L polycarbonate bottles and the total volume was filtered immediately through 0.2 μm Supor filters (Pall Gelman). The filters were stored in bead beater tubes and kept at -80°C until analysis. Samples were collected from four depths (200, 500, 650, and 850 dbar) at all SD stations, with the exception of station SD5 where seawater for DNA analyses was only collected at 500 dbar, and station SD14 where only 200 and 800 dbar were



analyzed. DNA was extracted using the Qiagen Plant kit, with additional freeze-thaw, bead beating, and Proteinase K steps for sample preparation before the kit purification, and elution to 100 μ L as previously described (Moisander et al., 2008). PCR was conducted using degenerate, nested *nifH* primers (Zehr et al., 2001), and the second round primers modified for Illumina library preparation, using a Bio-Rad C1000 thermocycler. The PCR mix was composed of 2.5 μ L of 10X Platinum Taq PCR buffer (Thermo Fisher), MgCl (2.5 mM final), dNTPs (0.2 mM final), primers (1 μ M final), 0.11 μ L Platinum Taq, and 4 μ L of DNA extract (1 μ L on second round), adjusted to 25 μ L total volume with nuclease free water. To alleviate PCR biases, PCR was conducted in triplicate in each round of reactions where first round triplicate reaction products were pooled, then 1 μ L was used as a template in triplicate reactions on the second round. A negative PCR control with water as template was included and treated in parallel with samples through all the subsequent steps. Sub-samples of the amplification products were checked via 1.2% TAE gel electrophoresis. The second round products showing a band of the expected size were pooled and purified using a magnetic bead protocol (Ampure, Beckman Coulter). The purified products were barcoded for Illumina (San Diego, CA, USA) MiSeq sequencing with Nextera indexes, using the manufacturer's protocol. The indexed products were purified again with magnetic beads, then quantified with a plate reader (Molecular Devices, Sunnyvale, CA, USA) using Picogreen (Thermo Fisher). The indexed samples were adjusted to equal concentrations and pooled for multiplexing during sequencing. The pooled sample was shipped to the Tufts University sequencing center (Boston, MA, USA) for paired end sequencing (2x300). The quality of the pooled sample and select individual samples was checked with a Bioanalyzer before the run. The resulting sequences were paired within Mothur (Schloss et al., 2009), and reads containing ambiguities or more than 8 homopolymers were discarded. The sequences were assigned to OTUs (at 97% cutoff) using the Uclust denovo picking method (Edgar, 2010) implemented in MacQIIME v1.9.1 (Caporaso et al., 2010). Low abundance OTUs consisting of less than 15 sequences across all samples were discarded from further processing. A representative sequence of each OTU was extracted from the data and quality processed in Arb (Ludwig et al., 2004), removing sequences that did not conceptually translate or were otherwise of poor quality. These OTUs were removed from further analysis. Remaining sequences were aligned based on protein alignment of the *nifH* fragments in a public *nifH* database (<https://www.jzehrlab.com/nifh>). Aligned protein sequences were assigned to *nifH* clusters using a decision tree statistical model, CART (Frank et al., 2016). The sequence data were normalized to proportion of total reads in each sample. Total relative abundances of sequences that fell in major *nifH* clusters were used to create a heatmap within R Studio using the VEGAN statistical package (Oksanen et al., 2015). Sequences were further classified through a locally run blastp using the *nifH* database as a reference (April 2015 database update). A neighbor joining tree was built in Arb with the 100 most abundant OTUs across all samples.



3 Results

3.1 Hydrography, nutrients, DOC and bacterial abundance

Sections of hydrographic variables (temperature, salinity), nutrients (NO_x -i.e. $\text{NO}_3^- + \text{NO}_2^-$ and PO_4^{3-}), DOC and bacterial abundance are shown in Fig. S1. All variables show a clear divide between the Melanesian Archipelago waters (MA; stations SD1 to SD12) and the South Pacific Gyre (GY; eastwards of SD12) (Moutin et al., 2017). Lower temperatures and salinity values ($<8^\circ\text{C}$ and ~ 35 , respectively) were measured below 450 to 600 dbar in the MA, while they were detected at shallower depths eastwards in the GY (Figs. S1a, b). Nutrient concentrations were high throughout the mesopelagic zone west of New Caledonia ($>30 \mu\text{M NO}_x$ and $>2 \mu\text{M PO}_4^{3-}$; and Figs. S1c, d). Sailing eastwards, NO_x in the MA region was $<5 \mu\text{M}$ between 150 and 250 dbar, with high concentrations $>30 \mu\text{M}$ being detected at ~ 680 dbar. Such high NO_x concentrations were detected at shallower depths (500 to 600 dbar) in the GY. PO_4^{3-} followed a similar pattern, with the highest concentrations detected at depths >500 dbar reaching $2.5 \mu\text{M}$.

DOC concentrations presented a pattern opposed to that of inorganic nutrients, with the <300 dbar presenting concentrations $50 - 60 \mu\text{M}$, lowering to $<40 \mu\text{M}$ below 600 dbar (Fig. S1e). Bacterial abundance was $>1 \times 10^5$ cells mL^{-1} down to 300 dbar in the MA waters, while its numbers decreased abruptly in the GY, especially east of SD12 (Fig. S1f)

3.2 High-resolution analysis of DOM (FTICRMS)

FTICRMS analysis of DOM yielded ~ 13500 molecular formulae in each sample, covering a mass range between 150 and 1000 Da. Each molecular formula was assigned to a given compound group as described in Seidel et al. (2014). According to this grouping, 4-31% of all compounds detected were oxygen-poor ($\text{O/C} < 0.5$) unsaturated aliphatics, 16% were oxygen-rich ($\text{O/C} > 0.5$) unsaturated aliphatics, 13% were polyphenols, while saturated fatty acids, sugars and peptides represented $<3\%$. Compounds usually regarded as labile DOM (peptides, sugars and saturated fatty acids) were relatively more abundant in the MA (data not shown).

3.3 Aphotic N_2 fixation rates

Aphotic N_2 fixation rates were measurable at all stations and depths and ranged between 0.05 and $0.68 \text{ nmol N L}^{-1} \text{ d}^{-1}$ (Fig. 1). These rates did not seem to follow any longitudinal or vertical pattern. However, the rates observed at station 13 (where a massive surface concentration of chlorophyll was observed; de Verneil et al., 2017) were on average ~ 5 -fold higher than at the other stations (average $0.63 \pm 0.07 \text{ nmol N L}^{-1} \text{ d}^{-1}$).

3.4 Diazotroph community composition



There were 3317-146864 (mean = 88867, s.d. = 42574) sequences per sample after pairing and the QA/QC steps. The negative control resulted in only 8 reads belonging to 6 OTUs. These sequences are likely a result of misbinning at the time of sequencing, and therefore the negative control was removed from downstream analysis. Shannon diversity at the 97% OTU level was not significantly affected by either depth or station (one-way ANOVA $p > 0.05$).

The majority of *nifH* sequences fell to Clusters 1 and 3, although Clusters 2 and 4 were represented in the transect at low relative abundances (Fig. 2). Within Cluster 1, subcluster 1G, which contains Gammaproteobacteria, accounted for over half of the total sequences (56%, s.d. = 38%). With a few exceptions, in samples with lower proportions of 1G, subcluster 3S was the most abundant group.

Cluster 3S had high relative abundances at station SD10 and in the 200 and 500 dbar depths of stations SD2 and SD12, as well as at 200 dbar at station SD13. The cyanobacterial subcluster 1B was observed at very low relative abundance throughout all stations and depths (average 0.5% of total community) and included *Trichodesmium*, UCYN-A, and *Richelia*. Consistent variations in community composition among depths and stations were not detected via cluster-based analysis, however, patterns emerged when observing data at the OTU level in abundant clusters (Fig. 3). In subcluster 1G, reads most closely matching an unclassified bacterium from the tropical North Atlantic (Unc12217, E value = 2.82×10^{-70} ; Table 1, Fig. 4) in the *nifH* database dominated the communities in the 650 dbar depth, and this phylotype was found only at minor proportions in other depths. This phylotype had an approximately 97% amino acid identity with *Vibrio diazotrophicus* (Fig. 4). This Unc12217/*V. diazotrophicus* related phylotype was present at high proportions across all other 650 dbar samples except at station SD2, the westernmost station. Although identified as “Other 1G” in Fig. 3, this trend was also true for several other groups present only at the 650 dbar depth (best matches with database sequences Unc12243, Unc12270, and UncPr491; Table 1). An additional group was found only at 650 dbar in the easternmost stations (SD10-SD13), closely matching a sequence from the Amazon River (UncM2163, E value = 4.22×10^{-74} ; Table 1). Within the *nifH* Cluster 3, subcluster 3S was the most widespread and abundant, with representation from three groups in the reference database: Unc12045, UncB2403, and UncMa132. Sequences with best matches with Unc12045 (Genbank ID: ADV51583; Turk et al., 2011), and UncB2403 (AAP48957; Steward et al., 2004) were present at stations SD2, SD4, SD10, and SD12, but had the highest relative abundance at station SD10, 500 dbar at station SD2, and the 200 and 500 dbar depths of station sd12. UncMa132 (AAS98182; unpublished) related groups were recovered from all stations at a low relative abundance, with the highest relative abundance in the 200 dbar samples from stations SD2, SD10, SD12, and SD13, and the 800 dbar samples from stations SD4 and SD10. These 3S groups have no closely related cultivated isolates, with the closest similarity with *Spirochaeta aurantia* (74-78% similarity, AF325792). All of the top 100 most abundant OTUs fell in Clusters 1 and 3 (Fig. 4). The majority fell in the Cluster 1G, with several additional phylotypes present in addition to the major ones discussed above. Several OTUs were closely related with previously described sequences



from the South Pacific Ocean mesopelagic layers (Benavides et al. 2015). *Magnetococcus* sp. and *Methylomonas* sp., and *Teredinibacter turnerae* were among closest cultivated representatives to Cluster 1G OTUs recovered (Fig. 4). Among the OTUs that fell in the Cluster 3, *Desulfovibrio* spp. were the closest cultivated representatives in the NCBI database.

5

3.5 N₂ fixation and diazotrophs related to in situ environmental parameters

Bonferroni-corrected Spearman rank correlations showed that N₂ fixation rates were only significantly correlated with temperature ($\rho = 0.263$, $p = 0.045$), salinity ($\rho = 0.284$, $p = 0.029$), and DOC concentrations ($\rho = 0.269$, $p = 0.042$; note that these hydrographic variables and DOC were
10 intercorrelated between them, data not shown; Table S1). A redundancy analysis (RDA; Fig. 5) including hydrographic variables, inorganic nutrients, DOC, bacterial abundance, N₂ fixation rates and DOM PCoA scores indicated that N₂ fixation rates were not related to DOM compositional variability (Table S1). Shallower samples such as those from 200 dbar were significantly related to temperature, salinity, oxygen and DOC concentrations, while the first principal coordinate of DOM related to the
15 majority of the samples. Stations SD13 and SD15 (easternmost part of the transect, within the GY) were partly related to depth and NO_x concentrations (samples from 650 and 800 dbar), while the rest of the samples of the profile appeared very distant in the RDA plot (Fig. 5).

4 Discussion

20 The aphotic N₂ fixation activity measured in the WTSP was low (average 0.18 ± 0.07 nmol N L⁻¹ d⁻¹), but consistently detected across all depths and stations (Fig. 1), representing on average 13 and 51% of photic N₂ fixation, in the MA and GY waters, respectively (Bonnet et al., submitted to this issue). It is pertinent to note that aphotic N₂ fixation rates may be underestimated if a significant percentage of the non-cyanobacterial diazotroph population is smaller than 0.7 μm (the nominal pore
25 size of GF/F filters), as N₂ fixation rates in non-cyanobacteria dominated environments is significantly higher when smaller pore size filters are used (Bombar et al., submitted). Aphotic N₂ fixation may contribute significantly to global fixed nitrogen inputs if widespread throughout the ocean's mesopelagic zone (or deeper). Unfortunately, our ability to assess this contribution remains hindered by the lack of specific N₂ fixation methods and our poor understanding of the ecophysiology of non-
30 cyanobacterial diazotrophs (Bombar et al., 2016; Moisander et al., 2017).

N₂ fixation rates in aphotic environments correlate with different DOM compound groups in different regions (Benavides et al., 2015; 2016), and *nifH* gene expression varies among non-cyanobacterial diazotroph phylotypes when exposed to conditions presumed to enhance their N₂ fixation activity (Severin et al., 2015). N₂ fixation was detected as low rates across an oligotrophic-to-
35 ultraoligotrophic transect in the WTSP. These rates were not significantly correlated to DOM compounds as identified by FTICRMS, despite they were positively correlated to DOC concentrations.



Non-cyanobacterial diazotroph communities are usually highly diverse in aphotic marine waters (e.g. Hewson et al., 2007). If such phylogenetic diversity also entails a broad metabolic diversity and different affinities for DOM compounds, correlations between DOM and non-cyanobacterial diazotroph abundance, identity and/or N₂ fixation activity will likely be blurred. Such ecophysiological heterogeneity may be also be reflected by the lack of longitudinal or vertical patterns in N₂ fixation rates observed along the transect (Fig. 1).

Some depth- and longitude related patterns were observed within the potential diazotroph community, one of the major patterns being a distinct *V. diazotrophicus* related phylotype from the major *nifH* subcluster 1G dominating at the 650 dbar depth. These sequences were unique from the 1G sequences found at other depths, and, with the exception of station SD2, were found uniformly across stations. A potential cause for the depth variation seen at 650 dbar is the presence of oxygenated Sub-Antarctic Mode Water (SAMW) at this depth (Fumenia et al., submitted to this issue). The high concentration of oxygen in this water mass (190-220 μmol kg⁻¹) could potentially shift the diazotroph community to members that can withstand higher levels of oxygen. To our knowledge, this is the first study identifying a relationship between *nifH* community composition and large-scale oceanographic circulation patterns in mesopelagic depths.

Members of the 1G subcluster include a variety of Gammaproteobacteria, and this group has previously been reported at high numbers in tropical surface waters including in the WTSP (Messer et al., 2017). In mesopelagic waters, transcripts from the 1G subcluster have been reported in an oxygen-deficient zone in the Arabian Sea at a depth of 175 m (Jayakumar et al., 2012), and genes have been reported from the WTSP from depths of 350-600 m (Benavides et al., 2015). Closely related cultivated isolates to the sequences found in this study include members of the Gammaproteobacterial genera *Vibrio*, *Pseudomonas*, *Klebsiella*, and *Agrobacterium*. The cyanobacterium *Pseudanabaena* also had relatively close relationship to the 650 dbar subcluster 1G sequences. When the proportion of sequences from subcluster 1G was low, members of cluster 3, primarily subcluster 3S, tended to have higher relative abundances (mostly east of the Tonga Trench, located between stations SD9 and SD10; Fig. S1). The three major matches of sequences in this study within the Arb database for subcluster 3S were of sequences reported from the surface waters in the North Pacific Subtropical Gyre and the Eastern North Atlantic, and a hypersaline lake. The phylotype most commonly observed at 200 dbar was most similar to sequences reported in the tropical North Pacific (AAS98182). Cluster 3 is typically considered to contain obligate and facultative anaerobes including *Spirochaeta* and *Desulfovibrio*. Cluster 3 diazotrophs were present in low gene copy numbers in North Atlantic surface waters, even when NO₃⁻ concentrations were high (Langlois et al., 2008). Members of Cluster 3 have also been recovered in the mesopelagic WTSP (Benavides et al., 2015), although this study reports longitudinal variation as a primary driver of Cluster 3 phylotype diversity and relative abundance.



The cyanobacterial subcluster 1B including *Trichodesmium*, UCYN-A, and *Richelia* was observed at very low relative abundance throughout all stations and depths (average 0.5% of total community), in agreement with the findings of Caffin et al. (2017), who detected those phylotypes in sediment traps deployed during the OUTPACE cruise at 150 and 325 m. Dead *Trichodesmium* colonies are thought to be mainly degraded in the photic zone (Letelier and Karl, 1998), although the detection of *Trichodesmium* in sediment traps and seawater samples obtained from the mesopelagic zone (Agusti et al., 2015; Chen et al., 2003) suggests that decayed dense blooms likely sink fast down the water column. The detection of cyanobacterial diazotroph *nifH* sequences in the mesopelagic zone questions whether the N₂ fixation rates measured are solely attributable to non-cyanobacterial diazotrophs (Moisander et al., 2017). Cyanobacterial photosynthetic diazotrophs reach the mesopelagic zone through sinking and sedimentation, and thus are unlikely diazotrophically active when devoid of light. However, recent studies have detected photosynthetically active diatoms at depths overpassing the mesopelagic zone (Agustí et al., 2015), indicating that dead cell packages can be exported vertically at high speed. If cyanobacterial diazotrophs remain active when they reach the aphotic layer, or if they die or shut down N₂ fixation on the way, remains an open question.

The data presented here are a significant contribution to the scarce availability of aphotic N₂ fixation rates, generally ocean wide, and specifically in the WTSP. Despite our knowledge on the ecophysiology of aphotic non-cyanobacterial diazotrophs is limited (Bombar et al., 2016), their ubiquity in the mesopelagic layer and the consistent detection of active N₂ fixation activity at all depths sampled during our study suggest that aphotic N₂ fixation may contribute significantly to fixed nitrogen inputs in this area.

Acknowledgements

This is a contribution of the OUTPACE (Oligotrophy from Ultra-oligoTrophy PACific Experiment) project (<https://outpace.mio.univ-amu.fr/>) funded by the French research national agency (ANR-14-CE01-0007-01), the LEFE-CYBER program (CNRS-INSU), the GOPS program (IRD), and the CNES (BC T23, ZBC 4500048836). The OUTPACE cruise (<https://doi.org/10.17600/15000900>) was managed by MIO (OSU Institut Pythéas, AMU) from Marseilles (France). The authors thank the crew of the R/V *L'Atalante* for outstanding on-ship operations. M.B. was funded by the People Programme (Marie Skłodowska-Curie Actions) of the European Union's Seventh Framework Programme (FP7/2007-2013) under REA grant agreement number 625185. NSF OCE-1733610 award to P.M. supported P.M. and K.S. S.D. was funded by the NSF award OCE-1434916 and received institutional support funded by the Vetlesen Foundation.



References

- Agustí, S., González-Gordillo, J. I., Vaqué, D., Estrada, M., Cerezo, M. I., Salazar, G., Gasol, J. M. and Duarte, C. M.: Ubiquitous healthy diatoms in the deep sea confirm deep carbon injection by the biological pump, *Nature Communications*, 6, 1–8, doi:10.1038/ncomms8608, 2015.
- 5 Benavides, M., Bonnet, S., Hernández, N., Martínez-Pérez, A. M., Nieto-Cid, M., Álvarez-Salgado, X. A., Baños, I., Montero, M. F., Mazuecos, I. P., Gasol, J. M., Osterholz, H., Dittmar, T., Berman-Frank, I. and Aristegui, J.: Basin-wide N₂ fixation in subsurface waters of the Mediterranean Sea, *Global Biogeochemical Cycles*, 30(6), 952–961, doi:10.1002/2015GB005326, 2016.
- Benavides, M., Moisaner, P. H., Berthelot, H., Dittmar, T., Grosso, O. and Bonnet, S.: Mesopelagic N₂ Fixation Related to Organic Matter Composition in the Solomon and Bismarck Seas (Southwest Pacific), *PLOS ONE*, 10(12), e0143775, doi:10.1371/journal.pone.0143775, 2015.
- 10 Bentzon-Tilia, M., Severin, I., Hansen, L. H. and Riemann, L.: Genomics and Ecophysiology of Heterotrophic Nitrogen-Fixing Bacteria Isolated from Estuarine Surface Water, *mBio*, 6(4), e00929–15, doi:10.1128/mBio.00929-15, 2015.
- 15 Berthelot, H., Benavides, M., Moisaner, P. H., Grosso, O. and Bonnet, S.: High-nitrogen fixation rates in the particulate and dissolved pools in the Western Tropical Pacific (Solomon and Bismarck Seas), *Geophys. Res. Lett.*, 59(2), 623, doi:10.1146/annurev-marine-120709-142819, 2017.
- Bombar, D., Paerl, R. W. and Riemann, L.: Marine Non-Cyanobacterial Diazotrophs: Moving beyond Molecular Detection, *Trends in Microbiology*, 24(11), 916–927, doi:10.1016/j.tim.2016.07.002, 2016.
- 20 Bonnet, S., Biegala, I. C., Dutrieux, P., Slemons, L. O. and Capone, D. G.: Nitrogen fixation in the western equatorial Pacific: Rates, diazotrophic cyanobacterial size class distribution, and biogeochemical significance, *Global Biogeochemical Cycles*, 23(3), GB3012, doi:10.1029/2008GB003439, 2009.
- Bonnet, S., Caffin, M., Berthelot, H. and Moutin, T.: Hot spot of N₂ fixation in the western tropical South Pacific pleads for a spatial decoupling between N₂ fixation and denitrification, *Proc Natl Acad Sci USA*, 201619514, doi:10.1073/pnas.1619514114, 2017.
- 25 Bonnet, S., Dekaezemacker, J., Turk-Kubo, K. A., Moutin, T., Hamersley, R. M., Grosso, O., Zehr, J. P. and Capone, D. G.: Aphotic N₂ Fixation in the Eastern Tropical South Pacific Ocean, *PLOS ONE*, 8(12), e81265, doi:10.1371/journal.pone.0081265.s001, 2013.
- 30 Bonnet, S., Guieu, C., Bruyant, F., PRASIL, O., Van Wambeke, F., Raimbault, P., Moutin, T., Grob, C., Gorbunov, M. Y. and Zehr, J. P.: Nutrient limitation of primary productivity in the Southeast Pacific (BIOCOPE cruise), *Biogeosciences*, 5(1), 215–225, 2008.
- Bonnet, S., Rodier, M., Turk-Kubo, K., Germineaud, C., Menkes, C., Ganachaud, A., Cravatte, S., Raimbault, P. and Campbell, E.: Contrasted geographical distribution of N₂ fixation rates and *nifH* 35 phylotypes in the Coral and Solomon Seas (southwestern Pacific) during austral winter conditions, *Global Biogeochemical Cycles*, 29(11), 1874–1892, doi:10.1002/2015GB005117, 2015.
- Caffin, M., Moutin, T., Foster, R. A., Bouruet-Aubertot, P., Doglioli, A. M., Berthelot, H., Grosso, O., Helias-Nunige, S., Leblond, N., Gimenez, A., Petrenko, A. A., de Verneil, A. and Bonnet, S.: Nitrogen budgets following a Lagrangian strategy in the Western Tropical South Pacific Ocean: the prominent role of N₂ fixation (OUTPACE cruise), *Biogeosciences Discuss.*, 1–34, doi:10.5194/bg-2017-468-RC1, 40 2017.
- Capone, D. G., Zehr, J. P., Paerl, H. W., Bergman, B. and Carpenter, E. J.: *Trichodesmium*, a globally



- significant marine cyanobacterium, *Science*, 276(5316), 1221–1229, doi:10.1126/science.276.5316.1221, 1997.
- Caporaso, J. G., Kuczynski, J., Stombaugh, J., Bittinger, K., Bushman, F. D., Costello, E. K., Fierer, N., Peña, A. G., Goodrich, J. K., Gordon, J. I., Huttley, G. A., Kelley, S. T., Knights, D., Koenig, J. E., Ley, R. E., Lozupone, C. A., McDonald, D., Muegge, B. D., Pirrung, M., Reeder, J., Sevinsky, J. R., Turnbaugh, P. J., Walters, W. A., Widmann, J., Yatsunenko, T., Zaneveld, J. and Knight, R.: correspondence, *Nature*, 7(5), 335–336, doi:10.1038/nmeth0510-335, 2010.
- Chen, Y., Chen, H. Y. and Lin, Y. H.: Distribution and downward flux of *Trichodesmium* in the South China Sea as influenced by the transport from the Kuroshio Current, *Mar Ecol Prog Ser*, 259, 47–57, 10 2003.
- Chien, Y. T. and Zinder, S. H.: Cloning, functional organization, transcript studies, and phylogenetic analysis of the complete nitrogenase structural genes (*nifHDK2*) and associated genes in the archaeon *Methanosarcina barkeri* 227, *Journal of Bacteriology*, 178(1), 143–148, 1996.
- Codispoti, L. A.: An oceanic fixed nitrogen sink exceeding 400 Tg N a⁻¹ vs the concept of homeostasis in the fixed-nitrogen inventory, *Biogeosciences*, 4(2), 233–253, doi:10.5194/bg-4-233-2007, 2007. 15
- de Verneil, A., Rousset, L., Doglioli, A. M., Petrenko, A. A. and Moutin, T.: The Fate of a Southwest Pacific Bloom: Gauging the impact of submesoscale vs. mesoscale circulation on biological gradients in the subtropics, *Biogeosciences Discuss.*, 1–25, doi:10.5194/bg-2017-84-AC2, 2017.
- Dittmar, T., Koch, B., Hertkorn, N. and Kattner, G.: A simple and efficient method for the solid-phase extraction of dissolved organic matter (SPE-DOM) from seawater, *Limnol. Oceanogr. Methods*, 6, 230–235, doi:10.4319/lom.2008.6.230, 2008. 20
- Edgar, R. C.: Search and clustering orders of magnitude faster than BLAST, *Bioinformatics*, 26(19), 2460–2461, doi:10.1093/bioinformatics/btq461, 2010.
- Farnelid, H. and Riemann, L.: Heterotrophic N₂-fixing bacteria: overlooked in the marine nitrogen cycle?, in *Nitrogen Fixation Research Progress*, edited by G. N. Couto, pp. 409–423, Nova Science Publishers, Inc., New York. 2008. 25
- Farnelid, H., Andersson, A. F., Bertilsson, S., Al-Soud, W. A., Hansen, L. H., Sørensen, S., Steward, G. F., Hagström, Å. and Riemann, L.: Nitrogenase gene amplicons from global marine surface waters are dominated by genes of non-cyanobacteria, edited by J. A. Gilbert, *PLOS ONE*, 6(4), e19223, doi:10.1371/journal.pone.0019223.t001, 2011. 30
- Fernández, C., Farías, L. and Ulloa, O.: Nitrogen Fixation in Denitrified Marine Waters, *PLOS ONE*, 6(6), e20539, doi:10.1371/journal.pone.0020539.t001, 2011.
- Frank, I. E., Turk-Kubo, K. A. and Zehr, J. P.: Rapid annotation of *nifH* gene sequences using classification and regression trees facilitates environmental functional gene analysis, *Environmental Microbiology Reports*, 8(5), 905–916, doi:10.5194/os-5-101-2009, 2016. 35
- Galloway, J. N., Dentener, F. J., Capone, D. G., Boyer, E. W., Howarth, R. W., Seitzinger, S. P., Asner, G. P., Cleveland, C. C., Green, P. A. and Holland, E. A.: Nitrogen cycles: past, present, and future, *Biogeochemistry*, 70(2), 153–226, 2004.
- Gruber, N. and Galloway, J. N.: An Earth-system perspective of the global nitrogen cycle, *Nature*, 40 451(7176), 293–296, doi:10.1038/nature06592, 2008.
- Halm, H., Lam, P., Ferdelman, T. G., Lavik, G., Dittmar, T., LaRoche, J., D'Hondt, S. and Kuypers, M.



- M.: Heterotrophic organisms dominate nitrogen fixation in the South Pacific Gyre, *ISME J*, 6, 1238–1249, doi:10.1038/ismej.2011.182, 2012.
- Hamersley, M. R., Turk, K. A., Leinweber, A., Gruber, N., Zehr, J. P., Gunderson, T. and Capone, D. G.: Nitrogen fixation within the water column associated with two hypoxic basins in the Southern California Bight, *Aquat. Microb. Ecol.*, 63(2), 193–205, doi:10.3354/ame01494, 2011.
- Herbland, A., Le Bouteiller, A. and Raimbault, P.: Size structure of phytoplankton biomass in the equatorial Atlantic Ocean, *Deep Sea Research Part A. Oceanographic Research Papers*, 32(7), 819–836, 1985.
- Hewson, I., Moisander, P. H., Achilles, K. M., Carlson, C. A., Jenkins, B. D., Mondragon, E. A., Morrison, A. E. and Zehr, J. P.: Characteristics of diazotrophs in surface to abyssopelagic waters of the Sargasso Sea, *Aquat. Microb. Ecol.*, 46, 15–30, doi:10.3354/ame046015, 2007.
- Jayakumar, A., Al-Rshaidat, M. M. D., Ward, B. B. and Mulholland, M. R.: Diversity, distribution, and expression of diazotroph *nifH* genes in oxygen-deficient waters of the Arabian Sea, *FEMS Microbiol Ecol*, 82(3), 597–606, doi:10.1111/j.1574-6941.2012.01430.x, 2012.
- 15 Jickells, T. D., Buitenhuis, E., Altieri, K., Baker, A. R., Capone, D., Duce, R. A., Dentener, F., Fennel, K., Kanakidou, M., LaRoche, J., Lee, K., Liss, P., Middelburg, J. J., Moore, J. K., Okin, G., Oschlies, A., Sarin, M., Seitzinger, S., Sharples, J., Singh, A., Suntharalingam, P., Uematsu, M. and Zamora, L. M.: A re-evaluation of the magnitude and impacts of anthropogenic atmospheric nitrogen inputs on the ocean, *Global Biogeochemical Cycles*, doi:10.1002/2016GB005586, 2017.
- 20 Kana, T. M., Darkangelo, C., Hunt, M. D., Oldham, J. B., Bennett, G. E. and Cornwell, J. C.: Membrane inlet mass spectrometer for rapid high-precision determination of N₂, O₂, and Ar in environmental water samples, *Anal. Chem.*, 66(23), 4166–4170, 1994.
- Koch, B. P. and Dittmar, T.: From mass to structure: an aromaticity index for high-resolution mass data of natural organic matter, *Rapid Commun. Mass Spectrom.*, 20(5), 926–932, doi:10.1002/rcm.2386, 25 2006.
- Langlois, R. J., Hummer, D. and LaRoche, J.: Abundances and distributions of the dominant *nifH* phylotypes in the northern Atlantic Ocean, *Appl Environ Microbiol*, 74(6), 1922–1931, doi:10.1128/AEM.01720-07, 2008.
- Langlois, R. J., LaRoche, J. and Raab, P. A.: Diazotrophic diversity and distribution in the tropical and 30 subtropical Atlantic Ocean, *Appl Environ Microbiol*, 71(12), 7910–7919, doi:10.1128/AEM.71.12.7910–7919.2005, 2005.
- Langlois, R., Großkopf, T., Mills, M., Takeda, S. and LaRoche, J.: Widespread Distribution and Expression of Gamma A (UMB), an Uncultured, Diazotrophic, γ -Proteobacterial *nifH* Phylotype, edited by L. J. Stal, *PLOS ONE*, 10(6), e0128912, doi:10.1371/journal.pone.0128912.s014, 2015.
- 35 Letelier, R. M. and Karl, D. M.: *Trichodesmium* spp. physiology and nutrient fluxes in the North Pacific subtropical gyre, *Aquat. Microb. Ecol.*, 15(3), 265–276, 1998.
- Loescher, C. R., Großkopf, T., Desai, F. D., Gill, D., Schunck, H., Croot, P. L., Schlosser, C., Neulinger, S. C., Pinnow, N., Lavik, G., Kuypers, M. M. M., LaRoche, J. and Schmitz, R. A.: Facets of diazotrophy in the oxygen minimum zone waters off Peru, *ISME J*, 8, 2180–2192, 40 doi:10.1038/ismej.2014.71, 2014.
- Ludwig, W., Strunk, O., Westram, R., Richter, L., Meier, H., Yadhukumar, Buchner, A., Lai, T., Steppi, S., Jobb, G., Förster, W., Brettske, I., Gerber, S., Ginhart, A. W., Gross, O., Grumann, S., Hermann, S.,



- Jost, R., König, A., Liss, T., Lüßmann, R., May, M., Nonhoff, B., Reichel, B., Strehlow, R., Stamatakis, A., Sutckmann, N., Vilbig, A., Lenke, M., Ludwig, T., Bode, A. and Schleifer, K.-H.: ARB: a software environment for sequence data, *Nucleic Acids Res*, 32(4), 1363–1371, doi:10.1093/nar/gkh293, 2004.
- Messer, L. F., Brown, M. V., Furnas, M. J., Carney, R. L., McKinnon, A. D. and Seymour, J. R.:
5 Diversity and Activity of Diazotrophs in Great Barrier Reef Surface Waters, *FMICB*, 8, 123,
doi:10.3389/fmicb.2016.01870, 2017.
- Messer, L. F., Mahaffey, C., Robinson, C. M., Jeffries, T. C., Baker, K. G., Isaksson, J. B., Ostrowski,
M., Doblin, M. A., Brown, M. V. and Seymour, J. R.: High levels of heterogeneity in diazotroph
10 diversity and activity within a putative hotspot for marine nitrogen fixation, *ISME J*, 1–15,
doi:10.1038/ismej.2015.205, 2015.
- Moisander, P. H., Beinart, R. A., Hewson, I., White, A. E., Johnson, K. S., Carlson, C. A., Montoya, J.
P. and Zehr, J. P.: Unicellular Cyanobacterial Distributions Broaden the Oceanic N₂ Fixation Domain,
Science, 327(5972), 1512–1514, doi:10.1126/science.1185468, 2010.
- Moisander, P. H., Beinart, R. A., Voss, M. and Zehr, J. P.: Diversity and abundance of diazotrophic
15 microorganisms in the South China Sea during intermonsoon, *ISME J*, 2(9), 954–967,
doi:10.1038/ismej.2008.51, 2008.
- Moisander, P. H., Benavides, M., Bonnet, S., Berman-Frank, I., White, A. E. and Riemann, L.: Chasing
after Non-cyanobacterial Nitrogen Fixation in Marine Pelagic Environments, *FMICB*, 8, 7608,
doi:10.1111/j.1574-6968.1997.tb12589.x, 2017.
- Moisander, P. H., Serros, T., Paerl, R. W., Beinart, R. A. and Zehr, J. P.: Gammaproteobacterial
20 diazotrophs and *nifH* gene expression in surface waters of the South Pacific Ocean, *ISME J*, 8(10),
1962–1973, doi:10.1038/ismej.2014.49, 2014.
- Montoya, J. P., Holl, C. M., Zehr, J. P., Hansen, A., Villareal, T. A. and Capone, D. G.: High rates of
N₂ fixation by unicellular diazotrophs in the oligotrophic Pacific Ocean, *Nature*, 430(7003), 1027–
25 1032, doi:10.1038/nature02824, 2004.
- Montoya, J. P., Voss, M., Kahler, P. and Capone, D. G.: A simple, high-precision, high-sensitivity
tracer assay for N₂ fixation, *Appl Environ Microbiol*, 62(3), 986–993, 1996.
- Moutin, T., Doglioli, A. M., de Verneil, A. and Bonnet, S.: Preface: The Oligotrophy to the UITra-
oligotrophy PACific Experiment (OUTPACE cruise, 18 February to 3 April 2015), *Biogeosciences*,
30 14(13), 3207–3220, doi:10.5194/bg-2017-63, 2017.
- Rahav, E., Bar-Zeev, E., Ohayon, S., Elifantz, H., Belkin, N., Herut, B., Mulholland, M. R. and
Berman-Frank, I.: Dinitrogen fixation in aphotic oxygenated marine environments, *FMICB*, 4(227), 1–
11, doi:10.3389/fmicb.2013.00227/abstract, 2013.
- Raimbault, P. and Garcia, N.: Evidence for efficient regenerated production and dinitrogen fixation in
35 nitrogen-deficient waters of the South Pacific Ocean: impact on new and export production estimates,
Biogeosciences, 5(2), 323–338, doi:10.5194/bg-5-323-2008, 2008.
- Schloss, P. D., Westcott, S. L., Ryabin, T., Hall, J. R., Hartmann, M., Hollister, E. B., Lesniewski, R.
A., Oakley, B. B., Parks, D. H., Robinson, C. J., Sahl, J. W., Stres, B., Thallinger, G. G., Van Horn, D.
J. and Weber, C. F.: Introducing mothur: Open-Source, Platform-Independent, Community-Supported
40 Software for Describing and Comparing Microbial Communities, *Appl Environ Microbiol*, 75(23),
7537–7541, doi:10.1128/AEM.01541-09, 2009.
- Seidel, M., Beck, M., Riedel, T. and Waska, H.: Biogeochemistry of dissolved organic matter in an



anoxic intertidal creek bank, *Geochimica et Cosmochimica Acta*, 140, 418–434,
doi:10.1016/j.gca.2014.05.038, 2014.

5 Severin, I., Bentzon-Tilia, M., Moisander, P. H. and Riemann, L.: Nitrogenase expression in estuarine bacterioplankton influenced by organic carbon and availability of oxygen, *FEMS Microbiol Lett*, doi:10.1093/femsle/fnv105, 2015.

Sohrin, R. and Sempéré, R.: Seasonal variation in total organic carbon in the northeast Atlantic in 2000–2001, *J Geophys Res*, 110(C10), C10S90, doi:10.1029/2004JC002731, 2005.

10 Stenegren, M., Caputo, A., Berg, C., Bonnet, S. and Foster, R. A.: Distribution and drivers of symbiotic and free-living diazotrophic cyanobacteria in the Western Tropical South Pacific, *Biogeosciences Discuss.*, 1–47, doi:10.5194/bg-2017-63-RC1, 2017.

Steward, G. F., Zehr, J. P., Jellison, R., Montoya, J. P. and Hollibaugh, J. T.: Vertical Distribution of Nitrogen-Fixing Phylotypes in a Meromictic, Hypersaline Lake, *Microb Ecol*, 47(1), 30–40, doi:10.1007/s00248-003-1017-8, 2004.

15 Turk, A. K., Rees, A. P., Zehr, J. P., Pereira, N., Swift, P., Shelley, R., Lohan, M., Woodward, E. M. S. and Gilbert, J.: Nitrogen fixation and nitrogenase (*nifH*) expression in tropical waters of the eastern North Atlantic, *ISME J*, 5(7), 1201–1212, doi:10.1038/ismej.2010.205, 2011.

Zehr, J. P., Waterbury, J. B., Turner, P. J., Montoya, J. P., Omoregie, E., Steward, G. F., Hansen, A. and Karl, D. M.: Unicellular cyanobacteria fix N₂ in the subtropical North Pacific Ocean, *Nature*, 412(6847), 635–637, 2001.

20



Tables

Table 1: Blastp identities to members of the 1G subcluster.

<i>nifH</i> ID	Accession number	Study	Location reported	Closest cultivated relative (Identity, E value)
UncM2172	ABV00657	Unpublished (Moisander/Subramaniam et al.)	Gulf of Guinea	<i>Vibrio diazotrophicus</i> (98%, 1e-71)
Unc12217	ADV51755	Turk et al. (2011)	Tropical Eastern N. Atlantic	<i>Agrobacterium tumefaciens</i> (83%, 4e-55)
Unc18425	BAN66776	Unpublished (Shiozaki et al.)	Northern S. China Sea	<i>Pseudomonas stutzeri</i> (86%, 1e-64)
Unc17727	ABV00657	Unpublished (Moisander/Subramaniam et al.)	Gulf of Guinea	<i>Klebsiella pneumoniae</i> (100%, 4e-95)
Unc11967	ADV35118	Unpublished (Olson and Lesser)	Florida Keys	<i>Pseudanabaena cf. persicina</i> (97%, 3e-78)
UncMa745	ABX39720	Moisander et al. (2008)	S. China Sea	<i>Pseudomonas stutzeri</i> (96%, 1e-70)
UncPr802	AEA49463	Fernandez et al. (2011)	Eastern S. Pacific	<i>Vibrio natriegens</i> (96%, 3e-74)
UncMa806	AAV60084	Langlois et al. (2005)	Atlantic Ocean	<i>Agrobacterium tumefaciens</i> (96%, 1e-70)
UncM2163	ABF21183	Unpublished (Hewson and Fuhrman)	Amazon River	<i>Vibrio diazotrophicus</i> (81%, 6e-55)
Unc12136	ADV51674	Turk et al. (2011)	Tropical Eastern N. Atlantic	<i>Agrobacterium tumefaciens</i> (96%, 2e-69)
Unc12270	ADV51808	Turk et al. (2011)	Tropical Eastern N. Atlantic	<i>Vibrio diazotrophicus</i> (79%, 1e-52)
UncMa747	ABX39731	Moisander et al. (2008)	S. China Sea	<i>Pseudomonas stutzeri</i> (84%, 6e-60)
Unc12551	ADO20633	Halm et al. (2012)	S. Pacific Gyre	<i>Pseudanabaena cf. persicina</i> (95%, 2e-70)
UncMa832	ABD62932	Unpublished (Foster et al.)	Atlantic Ocean	<i>Pseudomonas stutzeri</i> (84%, 5e-60)
Unc15356	AER93057	Unpublished (Lopez)	Mexican oasis system soil	<i>Pseudanabaena cf. persicina</i> (95%, 1e-78)
UncPr491	AEA49150	Fernandez et al. (2011)	Eastern S. Pacific	<i>Pseudanabaena cf. persicina</i> (98%, 3e-76)
Unc12243	ADV51781	Turk et al. (2011)	Tropical Eastern N. Atlantic	<i>Vibrio diazotrophicus</i> (80%, 2e-54)

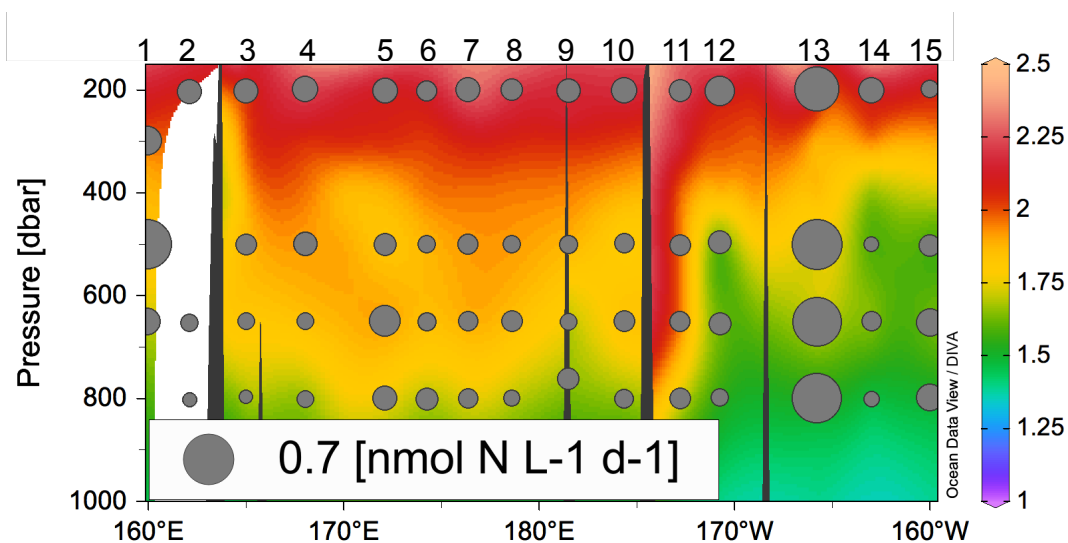
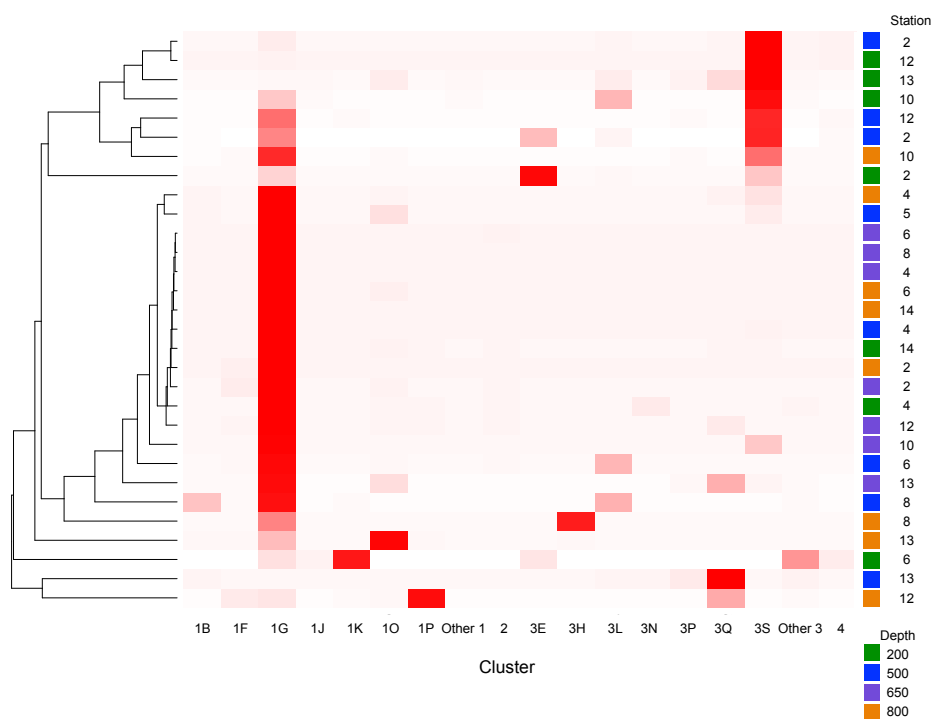


Figure 1: Longitudinal section of N_2 fixation ($\text{nmol N L}^{-1} \text{d}^{-1}$, as sized circles, reference size shown on the bottom left of the panel) superimposed on dissolved oxygen concentrations (color scale; mL L^{-1}). For reference, the station numbers are displayed on top of the panel.

5



5

Figure 2: Heatmap of *nifH* clusters and subclusters across the stations. The Bray-Curtis distances were used to build the dendrogram on the left. Distances were calculated with relative abundances of sequences by subcluster. Subclusters within Clusters 1 and 3 that had low relative abundances throughout all samples have been grouped as “other”.

10

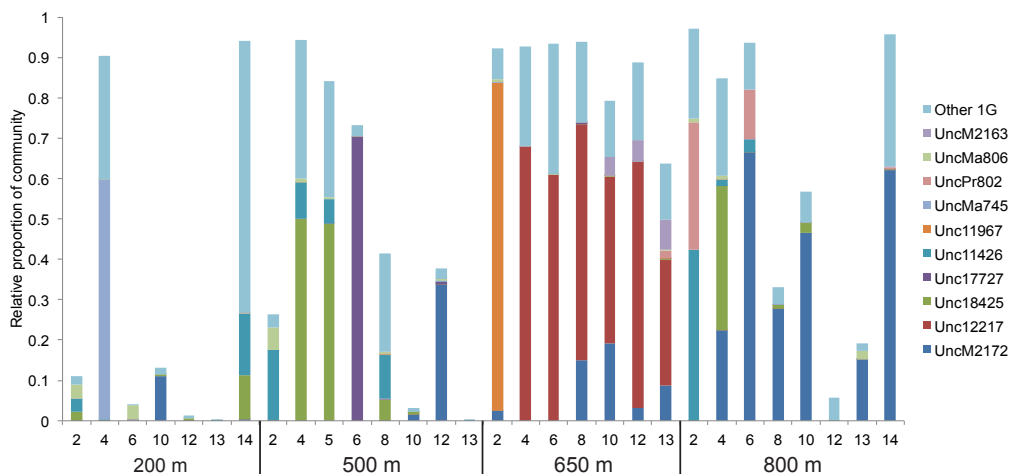


Figure 3: Relative abundance of subcluster 1G over depths and stations. Each bar represents the relative abundance of subcluster 1G in the total community for each sample. Samples are
 5 **arranged by station within each of the depths sampled. Blastp was used to assign OTUs to a top hit in the *nifH* reference database. The major sequence types in the *nifH* database found in the subcluster 1G are shown with different colors.**



Figure 4: A *nifH* amino acid neighbor-joining tree with 100 most abundant OTUs from this study shown. Sequences 'denovo-' shown in red are randomly chosen representative sequences from these OTUs (OTUs binned at 97% identity). The clusters in the tree are grouped at an approximately >95% sequence identity. The tree includes reference sequences (if uncultivated, names of these sequences start with 'Unc'). The reference sequences are shown with accession numbers from the *nifH* database and with the cluster identifier shown in blue if indicated in the *nifH* database. Additional sequences are included from a previous study in the South Pacific mesopelagic layers (Benavides et al. 2015); these clones are labeled with the original clone names M64XXAXX and depths.

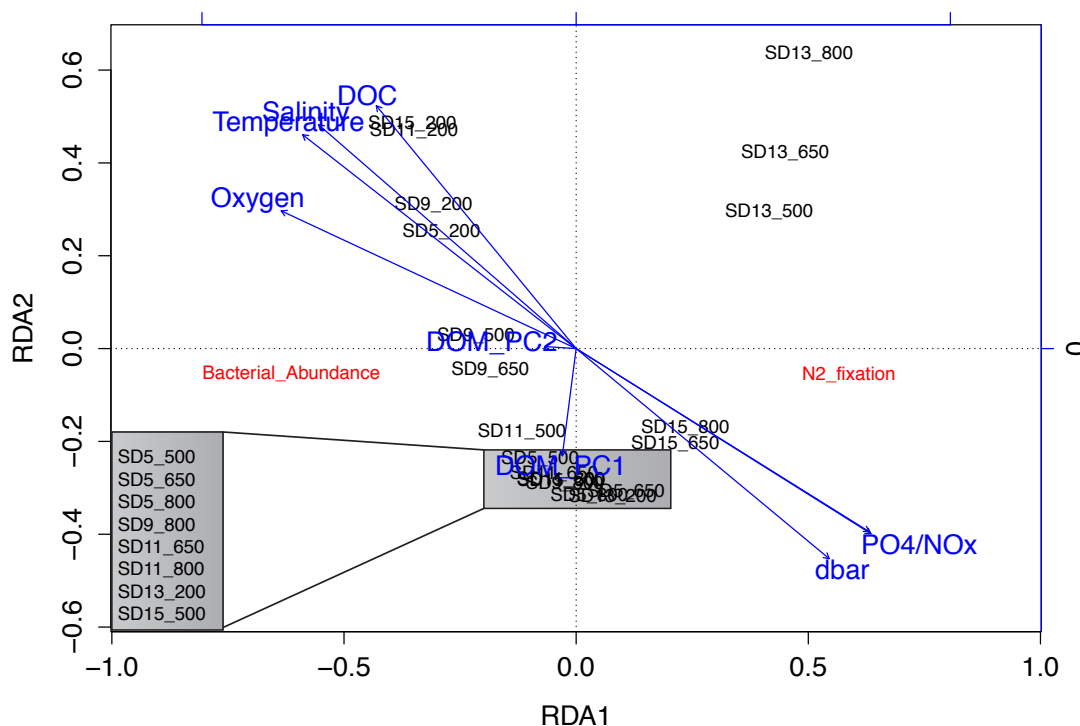


Figure 5: Redundancy analysis (RDA) ordination biplot showing the relationship between N_2 fixation rates, bacterial abundance, depth, environmental variables (temperature, salinity and oxygen), dissolved organic matter (DOM) principal coordinates, dissolved organic carbon (DOC) and inorganic nutrient concentrations.